The Impact of Interference Reflection on Reconfigurable Intelligent Surface-Aided Directional Transmissions

Yining Xu
Department of Electronic Engineering
Tsinghua University
Email: xu-yn16@mails.tsinghua.edu.cn

Sheng Zhou
Department of Electronic Engineering
Tsinghua University
Email: sheng.zhou@tsinghua.edu.cn

Zhisheng Niu
Department of Electronic Engineering
Tsinghua University
Email: niuzhs@tsinghua.edu.cn

2021 IEEE/CIC International Conference on Communications in China (ICCC) | 978-1-6654-4385-2/21/$31.00 ©2021 IEEE | DOI: 10.1109/ICCC52777.2021.9580353

***Abstract*—As a promising solution to deal with the blockage-sensitivity of millimeter wave band and to reduce the energy consumption caused by network densification, reconfigurable intelligent surface (RIS) shows good potential in improving the network performance. However, deploying large scale RISs leads to non-negligible reflection of interference, which may reduce the performance gain brought by RISs. In this paper, we investigate the coverage, spectrum efficiency and energy efficiency performance of a downlink directional transmission network with the aid of RISs using stochastic geometry. The numerical results show that deploying suitable density of RISs enhances the network performance while overly dense deployment brings performance degradation. We also find that the optimal RIS deployment fraction is a monotonically non-decreasing function of the blockage density and is monotonically non-increasing functions of the base station density and the beamwidth, which indicates that the deployment of RISs should be properly designed according to the network status instead of 'the more, the better'.**

***Index Terms*—Reconfigurable intelligent surface, directional transmissions, stochastic geometry.**

I. Introduction

As the needs for data-rate, seamless coverage and energy efficiency (EE) of the wireless communication network are ever increasing, some technologies attract researchers' attention, including millimeter wave (mmWave), ultra-dense network (UDN) and massive multiple-input multiple-output (MIMO). Yet the coverage demand can not always be met since mmWave is sensitive to the blockages due to its short wave length [1]. Also the energy consumption owing to network densification is still one of the vital problems to be solved [2]. Reconfigurable intelligent surface (RIS) is one of the promising technologies to deal with these problems due to its deployment flexibility and low energy cost characteristic. RIS is a near-passive transmission device, made of electronically controllable electromagnetic material, and the radio environment can be changed through adjusting the phase shifters [3]. When the RISs are used to provide reflected line-of-sight (LoS) links to the blocked users, the network coverage hole can be filled in, and the energy consumption can be reduced as compared with deploying equal amounts of base stations (BSs) or relays [4]. However, when the RISs are widely deployed in the network, the reflection of interference can not be neglected. Although the utilization of beamforming reduces the interference in the UDN network, how directional transmissions behave in the RIS-aided network is yet to study. Therefore, in this paper, we research the coverage, spectrum efficiency (SE) and EE performance of a downlink RIS-aided directional transmission network.

Among related works, ref. [5] considers a downlink RIS-aided non-orthogonal multiple access (NOMA) network, in which interference coefficient is used to approximate the actual reflected interference, and the results show that the achievable rate highly depends on the size of RIS. In [6], RIS passive beamformer is designed in order to cancel the interference and the performance analysis is derived. The results indicate that the SE and EE can be enhanced by increasing the number of RIS meta-surfaces. Ref. [7] considers a scenario that a part of the blockages in surroundings are co-located with RISs. However, it only investigates the coverage probability based on the path loss, while beamforming and interference are not considered. Ref. [8] studies coverage probability based on signal-to-interference-and-noise-ratio (SINR) in an RIS-aided mmWave network with uniform linear array (ULA) equipped in BSs and users. The network performance of two kinds of antenna schemes are analyzed respectively, in which the beam direction of the user can be either towards BSs or towards RISs. Ref. [9] also considers the ULA beamforming model and a total density constraint of BSs and RISs. Additionally, a two-step association scheme is proposed to minimize the uplink path loss from the serving BS to the RIS. In [9], the RISs are assumed to be deployed with a certain height and downwards to the ground to avoid multiple reflections. To the best of our knowledge, network performance analysis considering reflection of interference, sectored antenna model and association scheme based on average received desired signal strength is still missing. The contributions of our work

This work is sponsored in part by the National Key R&D Program of China No. 2020YFB1806605, by the Nature Science Foundation of China (No. 62022049, No. 61871254, No. 61861136003, No. 62111530197), by Open Research Fund Program of Beijing National Research Center for Information Science and Technology, and Hitachi Ltd.

can be summarized as follows:

- We consider a downlink RIS-aided network with directional transmissions. Especially, the reflection of interference is considered in our model. The expressions of network performance in terms of coverage, SE and EE are derived via stochastic geometry. We adopt a sectored antenna model to approximate the real beam pattern and an association scheme based on average received desired signal strength. The sum-distance path loss function is adopted for reflection in the mmWave band. And a distance-dependent LoS/ non-line-of-sight (NLoS) link model is used to imitate the sensitivity of mmWave to obstacles.
- The optimal RIS deployment fraction to maximize the network performance is found to be exist through the numerical results, which indicates that we should deploy the RISs properly instead of deploying as much RISs as possible.
- Additionally, network performance w.r.t RIS deployment fraction, blockage density, BS density and beam pattern are investigated and the characteristics of the optimal RIS deployment fraction are discussed. We observe that the optimal RIS deployment fraction is a monotonically non-decreasing function of blockage density, and is monotonically non-increasing functions of BS density and beamwidth.

The rest of the paper is organized as follows: the system model is elaborated in Sec. II and the theoretical results of system performance are derived in Sec. III. The discussions of the results are in Sec. IV and the conclusion is in Sec. V.

II. System Model

We assume that the locations of the BSs follow a homogeneous Poisson Point Process (HPPP) $\Phi_{BS} = \{B_i\} \in \mathbb{R}^2$ with density λ_{BS}. The blockages are modeled as line segments with equal length l, whose center points form another HPPP $\Phi_{BL} = \{L_i\} \in \mathbb{R}^2$ with density λ_{BL}. The angle between blockage L_i and the x-axis is denoted as ω_i, which is assumed to be uniformly distributed in $[0, 2\pi)$ and independently and identically distributed (i.i.d) for each $i \in \mathbb{Z}^+$. Therefore, the LoS probability of any path with communication distance r is $p_L(r) = \exp(-\beta r)$, where $\beta = \frac{2l\lambda_{BL}}{\pi}$ [1]. Let $\mathbb{I}_L(r)$ be the LoS indicator function of an arbitrary communication path with distance r, and we have:

$$\mathbb{I}_L(r) = \begin{cases} 1 & \text{w.p. } p_L(r) \\ 0 & \text{w.p. } 1 - p_L(r). \end{cases} \tag{1}$$

A fraction of the blockages are co-located with RISs and RISs are deployed on one of the two surfaces of the blockages. The set of center points of RISs $\Phi_R = \{R_i\} \in \mathbb{R}^2$ is a thinning HPPP of Φ_{BL}, whose density is $\lambda_R = \mu\lambda_{BL}$ with RISs deployment fraction $\mu \in [0, 1]$. To be notice, multiple reflections are not considered.

For a BS-user equipment (UE) direct link, the path loss is $P_d(r_{BU}) = r_{BU}^{-\alpha}$, where α is the path loss exponent and r_{BU} is the distance between BS and user. For a BS-RIS-UE reflected link, since the size of RIS element is sufficiently large as compared with mmWave wavelength, the RIS is considered as an 'anomalous mirror' and the sum-distance path loss function is adopted [10]. On the other hand, signal suffers energy loss from reflection on RIS due to non-ideal characteristics of device. The reflection power attenuation coefficient is denoted as γ. Thus, the path loss of a reflected link is $P_r(r_{BR} + r_{RU}) = \gamma(r_{BR} + r_{RU})^{-\alpha}$, where r_{BR} and r_{RU} are the distance between BS and RIS and the distance between RIS and user, respectively. Therefore, the equivalent link distance of a reflected link is the sum of distance of BS-RIS link and RIS-UE link. We assume an i.i.d. Rayleigh fading, denoted as $h \sim \exp(1)$, for an arbitrary link for tractability.

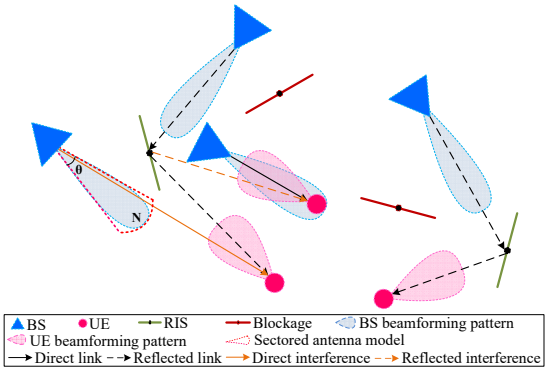

Fig. 1: Direct link, reflected link and interference in the RIS-aided directional transmissions.

We approximate the beamforming pattern to a sectored antenna model with negligible side-lobe gain, as illustrated in Fig. 1. The beamforming pattern is determined by the main lobe gain N_j and beamwidth θ_j with $j = \{\mathrm{B}, \mathrm{U}\}$ representing BS and user, respectively. The N_j and θ_j satisfies the equation $N_j\theta_j = 2\pi P_j$, where P_j is the transmission/received power for $j = \{\mathrm{B}, \mathrm{U}\}$, respectively. The power consumption of an RIS aroused by the phase shifters is P_R. Without loss of generality, we focus on the performance of a typical user, which is located at the origin. The beam directions of the typical user and its serving BS are aligned with each other in their direct link, while their beam directions are aligned to the RIS in the reflected link as shown in the Fig. 1. Overall, the total beamforming gain from the serving BS to the typical user is $N_B N_U$. Similarly, the total beamforming gain G from an arbitrary interfering BS, either a direct interfering BS or a reflected interfering BS, to the typical user has the following distribution:

$$G = \begin{cases} N_B N_U & \text{w.p. } \frac{\theta_B \theta_U}{4\pi^2} \\ 0 & \text{w.p. } 1 - \frac{\theta_B \theta_U}{4\pi^2}. \end{cases} \tag{2}$$

Additionally, we assume the RIS does not provide power gain in the reflection as power amplifier is not equipped.

The typical user associates to the serving BS according to the highest average received desired signal strength policy, i.e.,

choose a feasible LoS link with the lowest average path loss. The feasible LoS link includes two types: 1) *feasible LoS direct link:* the LoS direct BS-UE link; 2) *feasible LoS reflected link:* both BS-RIS and RIS-UE links are LoS. Additionally, the typical user and the serving BS are on the reflection side of the RIS. Therefore, the serving BS B^* satisfies the following condition:

$$B^*= \arg\max_{B_i\in\Phi_{BS}} \max_{B_i\in\Phi_{BS}}\left(\mathbb{I}_L(r_{B_i})P_d(r_{B_i}), \max_{R_k\in\Phi_R}\mathbb{I}_L(r_{B_iR_k})\mathbb{I}_L(r_{R_k})\delta_{B_iR_k}P_r(r_{B_iR_k}+r_{R_k})\right), \tag{3}$$

where r_{B_i}, r_{R_k} and $r_{B_iR_k}$ are the distances between the typical user and BS B_i, the distance between typical user and RIS R_k, the distance between BS B_i and RIS R_k, respectively. And $\delta_{B_iR_k}=1$ represents that a feasible reflected link exists, composed of the typical user, BS B_i and RIS R_k. Otherwise, $\delta_{B_iR_k}=0$. The probability distribution of $\delta_{B_iR_k}$ will be given in the next section.

The received SINR of the typical user is:

$$\mathrm{SINR}=\frac{N_BN_Uh\left[\mathbb{I}_L(r_{B^*})P_d(r_{B^*})+(1-\mathbb{I}_L(r_{B^*}))P_r(r_{B^*R^*}+r_{R^*})\right]}{\sigma^2+I_d+I_r}, \tag{4}$$

where

$$R^*= \arg\max_{R_k\in\Phi_R}\mathbb{I}_L(r_{B^*R_k})\mathbb{I}_L(r_{R_k})\delta_{B^*R_k}P_r(r_{B^*R_k}+r_{R_k}), \tag{5}$$

$$I_d=\sum_{i:B_i\in\Phi_{BS}\setminus\{B^*\}}\mathbb{I}_L(r_{B_i})P_d(r_{B_i})Gh, \tag{6}$$

$$I_r=\sum_{i:B_i\in\Phi_{BS}\setminus\{B^*\}}\sum_{k:R_k\in\Phi_R}\mathbb{I}_L(r_{B_iR_k})\mathbb{I}_L(r_{R_k})\delta_{B_iR_k}P_r(r_{B_iR_k}+r_{R_k})Gh. \tag{7}$$

Here σ^2 is the noise power normalized by the transmit power, and R^* is the serving RIS when a reflected link is chosen by the typical user for association. While I_d and I_r are the interference caused by the interfering BSs through direct links and reflected links, respectively.

III. Theoretical Results

In this paper, the main performance metrics are as follows:

i. The coverage probability $\mathcal{P}=\mathbb{P}[\mathrm{SINR}>\mathrm{T}]$, which is the probability that the received SINR of the typical user exceeds a threshold.
ii. The constrained area spectral efficiency (ASE) $\mathcal{A}=\lambda_{BS}\mathbb{E}[\log_2(1+\mathrm{SINR})\mathbb{I}\{\mathrm{SINR}>\mathrm{T}\}]$, which is the average throughput per unit area and frequency, where $\mathbb{I}\{\cdot\}$ is the indication function.
iii. The EE $\mathcal{E}=\mathcal{A}/(\lambda_{BS}P_B+\lambda_RP_R)$, which is the throughput per unit power and frequency.

Since the expression of constrained ASE can be directly obtained form the coverage probability as:

$$\mathcal{A}=\frac{\lambda_{BS}}{\ln 2}\int_{\ln(1+T)}^{\infty}\mathbb{P}[\mathrm{SINR}>e^t-1]\mathrm{d}t+\lambda_{BS}\log_2(1+T)\mathbb{P}[\mathrm{SINR}>T], \tag{8}$$

and the expression of EE can be obtained sequentially, we mainly focus on the derivation of coverage probability in the following parts.

According to our association policy, there are three kinds of association modes: 1) BS-UE direct association; 2) BS-RIS-UE reflected association; 3) user does not have any available association BS. We denote the probability of this three situations as $\mathcal{X}_d$, $\mathcal{X}_r$ and $\mathcal{X}_0$, respectively. The following expressions can be obtained from [7] with some variable modifications:

$$\mathcal{X}_0=\exp\left(-2\pi\lambda_{BS}\cdot\int_0^{\infty}\left(p_L(u)+(1-p_L(u))\left(1-\exp\left(-\lambda_R\int_{-\pi}^{\pi}\int_0^{\infty}g(u,v,\psi)v\mathrm{d}v\mathrm{d}\psi\right)\right)\right)u\mathrm{d}u\right), \tag{9}$$

$$\mathcal{X}_d=\int_0^{\infty}f_d(r)\exp\left(-2\pi\lambda_{BS}\int_0^{\infty}(1-p_L(u))F_r(r\gamma^{\frac{1}{\alpha}},u)u\mathrm{d}u\right)\mathrm{d}r, \tag{10}$$

$$\mathcal{X}_r=1-\mathcal{X}_0-\mathcal{X}_d, \tag{11}$$

where

$$f_d(x)=2\pi x\lambda_{BS}\exp\left(-\beta x-2\pi\lambda_{BS}\frac{1}{\beta_2}(1-(\beta x+1)\exp(-\beta x))\right), \tag{12}$$

$$F_r(x,u)=\begin{cases}1-\exp\left(-\lambda_R\int_{-\pi}^{\pi}\int_0^{\frac{x^2-u^2}{2(x-u\cos\psi)}}g(u,v,\psi)v\mathrm{d}v\mathrm{d}\psi\right) & \text{if } x\geq u\\ 0 & \text{otherwise}\end{cases}, \tag{13}$$

with

$$g(u,v,\psi)=\frac{1}{2}p_L(v)p_L\left(\sqrt{u^2+v^2-2uv\cos(\psi)}\right)\cdot\left(1-\frac{1}{\pi}\cos^{-1}\left(\frac{v-u\cos(\psi)}{\sqrt{u^2+v^2-2uv\cos(\psi)}}\right)\right). \tag{14}$$

The function $g(u,v,\psi)$ is the probability that the reflected LoS link is feasible, which means the BS and the typical user lie on the reflection side of the RIS and the reflected link is LoS. It also reveals that the probability distribution of $\delta_{B_iR_k}$ is :

$$\delta_{B_iR_k}=\begin{cases}1 & \text{w.p. } \frac{1}{2}-\frac{1}{2\pi}\cos^{-1}\left(\frac{v-u\cos(\psi)}{\sqrt{u^2+v^2-2uv\cos(\psi)}}\right)\\ 0 & \text{w.p. } \frac{1}{2}+\frac{1}{2\pi}\cos^{-1}\left(\frac{v-u\cos(\psi)}{\sqrt{u^2+v^2-2uv\cos(\psi)}}\right)\end{cases}, \tag{15}$$

where the distance between the BS B_i and the typical user is u, the distance between the RIS R_k and the typical user is v and the angle between the UE-BS link and UE-RIS link is ψ. The function $f_d(x)$ is the probability density function (PDF) of the distance between the nearest LoS BS and the typical user. The function $F_r(x,u)$ is the probability distribution of the distance of the shortest reflected link condition on that the distance between the typical user and the association BS is

Theorem 1. *The coverage probability of the RIS-aided mmWave network with directional transmissions is*

$$\mathcal{P}=\mathcal{X}_d\int_0^{\infty}\exp\left(-\frac{T\sigma^2}{N_BN_UP_d(r)}\right)\mathcal{L}_{I_d}^{d}\mathcal{L}_{I_r}^{d}f_d(r)\mathrm{d}r+\mathcal{X}_r\int_0^{\infty}\exp\left(-\frac{T\sigma^2}{N_BN_UP_r(t)}\right)\mathcal{L}_{I_d}^{r}\mathcal{L}_{I_r}^{r}f_r(t)\mathrm{d}t,$$

where the functions $\mathcal{L}_{I_d}^{d}$, $\mathcal{L}_{I_r}^{d}$, $\mathcal{L}_{I_d}^{r}$ *and* $\mathcal{L}_{I_r}^{r}$ *are given by*

$$\mathcal{L}_{I_d}^{d}=\exp\left(-2\pi\lambda_{BS}\int_r^{\infty}\frac{\theta_B\theta_U}{4\pi^2}\frac{TP_d(r_i)p_L(r_i)}{P_d(r)+TP_d(r_i)}\,r_i\mathrm{d}r_i\right),$$

$$\mathcal{L}_{I_r}^{d}=\exp\left(-2\pi\lambda_{BS}\int_0^{\infty}\left(1-\exp\left(-2\pi\lambda_R\int_{-\pi}^{\pi}\int_{R_1}^{\infty}\frac{\theta_B\theta_U}{4\pi^2}\frac{g(r_i,r_k,\psi)TP_r(\sqrt{r_i^2+r_k^2-2r_ir_k\cos\psi}+r_k)}{P_d(r)+TP_r(\sqrt{r_i^2+r_k^2-2r_ir_k\cos\psi}+r_k)}r_k\mathrm{d}r_k\mathrm{d}\psi\right)\right)r_i\mathrm{d}r_i\right),$$

$$\mathcal{L}_{I_d}^{r}=\exp\left(-2\pi\lambda_{BS}\int_{t\gamma^{-\frac{1}{\alpha}}}^{\infty}\frac{\theta_B\theta_U}{4\pi^2}\frac{TP_d(r_i)p_L(r_i)}{P_r(t)+TP_d(r_i)}\,r_i\mathrm{d}r_i\right),$$

$$\mathcal{L}_{I_r}^{r}=\exp\left(-2\pi\lambda_{BS}\int_0^{\infty}\left(1-\exp\left(-2\pi\lambda_R\int_{-\pi}^{\pi}\int_{R_2}^{\infty}\frac{\theta_B\theta_U}{4\pi^2}\frac{g(r_i,r_k,\psi)TP_r(\sqrt{r_i^2+r_k^2-2r_ir_k\cos\psi}+r_k)}{P_r(t)+TP_r(\sqrt{r_i^2+r_k^2-2r_ir_k\cos\psi}+r_k)}r_k\mathrm{d}r_k\mathrm{d}\psi\right)\right)r_i\mathrm{d}r_i\right),$$

where $R_1=\max\left\{\frac{r_i^2-(r\gamma^{1/\alpha})^2}{2\left(r_i\cos\psi-r\gamma^{1/\alpha}\right)},0\right\}$ *and* $R_2=\max\left\{\frac{r_i^2-t^2}{2(r_i\cos\psi-t)},0\right\}$. *The functions* $\mathcal{X}_d$, $\mathcal{X}_r$, $f_d(x)$ *and* $f_r(x)$ *are already given in equalities (10), (11), (12) and (16).*

Proof. See Appendix A. □

u. Similarly, the PDF of the distance of the shortest reflected link is calculated as:

$$f_r(x)=2\pi\lambda_{BS}\exp\left(-2\pi\lambda_{BS}\int_0^{x}(1-p_L(u))F_r(x,u)u\mathrm{d}u\right)\cdot\int_0^{x}(1-p_L(u))\frac{\partial F_r(x,u)}{\partial x}u\mathrm{d}u, \tag{16}$$

where

$$\frac{\partial F_r(x,u)}{\partial x}=\lambda_R\exp\left(-\lambda_R\int_{-\pi}^{\pi}\int_0^{\frac{x^2-u^2}{2(x-u\cos\psi)}}g(u,v,\psi)v\mathrm{d}v\mathrm{d}\psi\right)\cdot\int_{-\pi}^{\pi}g\left(u,\frac{x^2-u^2}{2\left(x-u\cos\psi\right)},\psi\right)\frac{(x^2-2ux\cos\psi+u^2)(x^2-u^2)}{4(x-u\cos\psi)^3}\mathrm{d}\psi. \tag{17}$$

The full expression of the coverage probability is given in Theorem 1 on the top of the page.

IV. Numerical Results and Discussion

In this section, we provide some numerical results to evaluate the system performance w.r.t key parameters, including blockage density λ_{BL}, BS density λ_{BS}, RIS deployment fraction μ and beamwidth θ_B and θ_U. The default system parameters are: $\alpha=4$, $\gamma=0.85$, $l=15$m, $\sigma^2=10^{-8}$, $T=3$dB, $\lambda_{BS}=10$BSs/km^2, $\lambda_{BL}=500$Blockages/km^2, $N_B=20$dB, $\theta_B=30$degs, $N_U=10$dB and $\theta_U=90$degs. For the energy consumption parameter, we assume $P_B=39.2$dBm and $P_R=15$dBm.

Fig. 2 shows the coverage probability, constrained ASE and EE for different values of RIS deployment fraction and blockage density. We find that the optimal RIS deployment fraction, which is marked with star in the figure, increases as the blockage density increases. When the blockage density is small, e.g. $\lambda_{BL}=100$Blockages/km^2, most of the users in the network associates to the serving BS through a direct link. Thus, deploying more RISs provides minor gain on the desired signal enhancement, but the total interference is greatly enlarged by the reflection. However, when the network has intensive blockages and most of the BS-UE links are blocked, deploying appropriate amount of RISs enhances the performance notably as the RISs provide another communi-

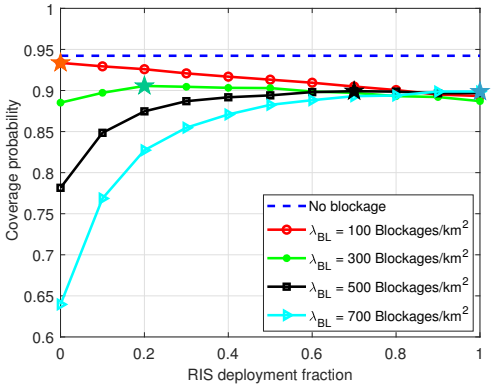

(a) Coverage probability w.r.t RIS deployment fraction

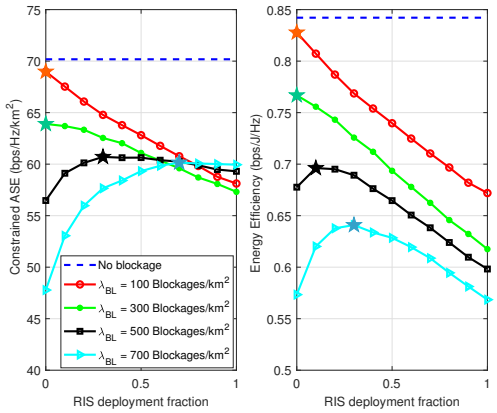

(b) Constrained ASE and EE w.r.t RIS deployment fraction

Fig. 2: Coverage probability $\mathcal{P}$, constrained ASE $\mathcal{A}$ and EE $\mathcal{E}$ scaling with RIS deployment fraction μ under different blockage density λ_{BL}.

cation links to the NLoS users, and the impact of reflected interference is compensated in comparison. Especially, EE performance highly depends on the ratio P_B/P_R, which indicates that we should deploy more RISs when deploying RISs is 'energy-economical'. In addition, comparing Fig. 2(a) with Fig. 2(b), the coverage-optimal RIS deployment fraction is different from the ASE-optimal and the EE-optimal RIS deployment fraction, which leads to trade-offs between the coverage, SE and EE performance when designing the RIS deployment policy.

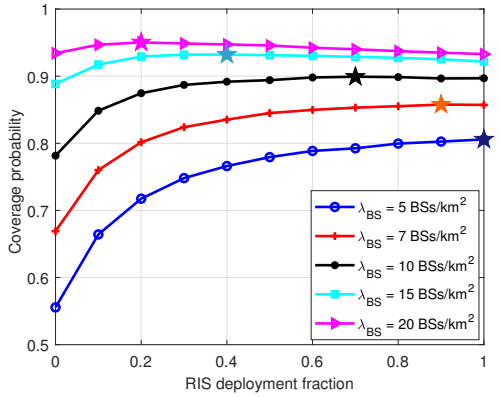

(a) Coverage probability w.r.t RIS deployment fraction

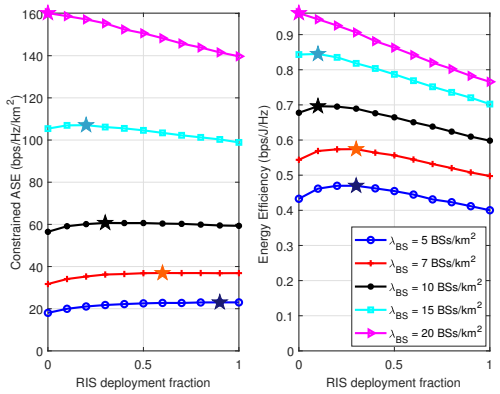

(b) Constrained ASE and EE w.r.t RIS deployment fraction

Fig. 3: Coverage probability $\mathcal{P}$, constrained ASE $\mathcal{A}$ and EE $\mathcal{E}$ scaling with RIS deployment fraction μ under different BS density λ_{BS}.

In Fig. 3, we plot the network performance as a function of RIS deployment fraction under varying BS density. We observe that deploying denser BSs improve the network performance as the average link distance is shortened when the BS density is not overly large. Similar to the insights of the Fig. 2, deploying more RISs even bring performance degradation under large BS density since the BS-UE direct link dominates the association links. While when BSs are sparsely deployed, utilizing RISs enhances the performance. The optimal RIS deployment fraction is a monotonically non-increasing function of the BS density as shown in the figure. In a word, the greater the ratio of blockage density to BS density, the better the performance of RISs, and the denser RISs should be.

In Fig.4, we investigate the network performance w.r.t RIS deployment fraction under different beamwidth. The EE performance w.r.t beamwidth is equivalent to the constrained ASE performance w.r.t the beamwidth since changing the beam pattern does not influence the energy consumption according to our model. The impact of RIS deployment fraction is much smaller than the impact of beamwidth to the coverage probability, constrained ASE and EE. Correspondingly, the optimal RIS deployment fraction increases as the beam becomes narrower. And for a relatively wide beam, e.g. $\theta_B = 90$degs and $\theta_U = 270$degs, the performance decreases even when the RIS deployment fraction is quite small. These results indicate that the reflected interference caused by the RIS dominates the performance, as the reflected interference is more likely to lie in the receive range of user when the beam is wide. Therefore, in the RIS-aided network, directional transmissions with relatively narrow beam is preferred to guarantee the network performance.

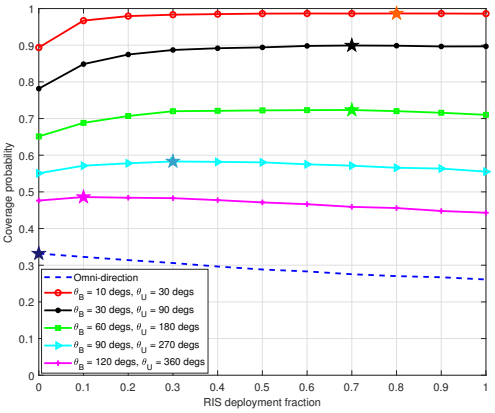

(a) Coverage probability w.r.t RIS deployment fraction

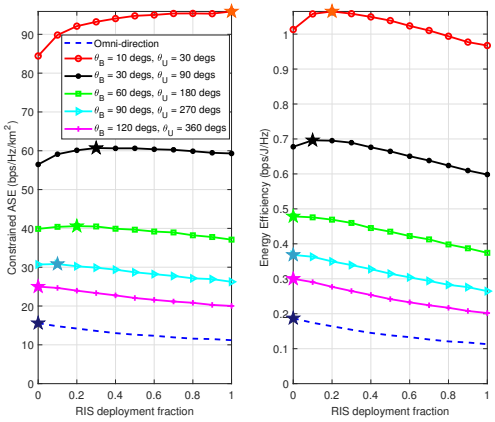

(b) Constrained ASE and EE w.r.t RIS deployment fraction

Fig. 4: Coverage probability $\mathcal{P}$, constrained ASE $\mathcal{A}$ and EE $\mathcal{E}$ scaling with RIS deployment fraction μ under different beamwidth θ_B and θ_U.

V. Conclusion

In this paper, we have investigated the coverage, SE and EE performance of a downlink directional transmission network when RISs are used to supply additional LoS reflected links in the scenario with full of blockages. We have considered that the RISs reflect not only the desired signal but also the interference to the users. The expressions of coverage probability, constrained ASE and EE are derived using stochastic

geometry. The results indicate that, in some cases, deploying dense RISs will in fact bring performance loss when reflection of interference is considered. Furthermore, we also find that the optimal RIS deployment fraction is a monotonically non-decreasing function of the blockage density and is monotonically non-increasing functions of the BS density and the beamwidth. And comparing to the RIS density, the beam pattern affects the performance more significantly. Then, since the optimal RIS density to maximize the coverage, SE and EE is different, the RIS deployment should be designed according to the specific optimization objective. Finally, interference cancellation schemes and proper beamformer design should be premeditated to lower down the interference in the RIS-aided network in future researches.

Appendix A: Proof of Theorem 1

Obviously, the coverage probability can be calculated as:

$$\mathcal{P}=\mathcal{X}_d\mathbb{P}\left[\frac{N_B N_U h P_d(r_{B^*})}{\sigma^2+I_d^d+I_r^d}>T\right]+\mathcal{X}_r\mathbb{P}\left[\frac{N_B N_U h P_r(r_{B^*R^*}+r_{R^*})}{\sigma^2+I_d^r+I_r^r}>T\right], \tag{18}$$

where I_d^d and I_r^d are the interference from direct links and reflected links to the association direct link, while I_d^r and I_r^r are the interference from direct links and reflected links to the association reflected link. The first probability term can be further expressed as:

$$\begin{aligned}\mathbb{P}\left[\frac{N_B N_U h P_d(r_{B^*})}{\sigma^2+I_d^d+I_r^d}>T\right] &\overset{(a)}{=}\int_0^\infty \mathbb{P}\left[h>\frac{T(\sigma^2+I_d^d+I_r^d)}{N_B N_U P_d(r)}\middle| r\right] f_d(r)\mathrm{d}r\\ &\overset{(b)}{=}\int_0^\infty \exp\left(-\frac{T\sigma^2}{N_B N_U P_d(r)}\right)\mathcal{L}_{I_d}^d\mathcal{L}_{I_r}^d f_d(r)\mathrm{d}r,\end{aligned} \tag{19}$$

where in (a), we use r instead of r_B^* as the distance of the association direct link for simplicity. Equality (b) follows from the exponential distribution of h. Then we take the major steps of the proof of $\mathcal{L}_{I_r}^d$ for example. The expressions of $\mathcal{L}_{I_d}^d, \mathcal{L}_{I_d}^r$ and $\mathcal{L}_{I_r}^r$ can be obtained through similar process.

The function $\mathcal{L}_{I_r}^d$ is the Laplace transform of the interference from reflected links when the typical user is associated to a direct link, which is expressed as:

$$\begin{aligned}&\mathcal{L}_{I_r}^d\\ &\overset{(c)}{=}\mathbb{E}_{\tilde{\Phi}_{BS}\tilde{\Phi}_R}\left[\prod_{i:B_i\in\tilde{\Phi}_{BS}}\prod_{k:R_k\in\tilde{\Phi}_R}\mathbb{E}_{G,h}\left[\exp\left(-\frac{TGhP_r(d+r_k)\mathbb{I}_L(d)\mathbb{I}_L(r_k)\delta_{B_iR_k}}{N_B N_U P_d(r)}\right)\right]\right]\\ &\overset{(d)}{=}\mathbb{E}_{\tilde{\Phi}_{BS}\tilde{\Phi}_R}\left[\prod_i\prod_k\mathbb{E}_{G,h}\left[\exp\left(-\frac{TGhP_r(d+r_k)}{N_B N_U P_d(r)}\right)g(r_i,r_k,\psi)+1-g(r_i,r_k,\psi)\right]\right]\\ &\overset{(e)}{=}\mathbb{E}_{\tilde{\Phi}_{BS}\tilde{\Phi}_R}\left[\prod_i\prod_k\left(1-\frac{g(r_i,r_k,\psi)TP_r(d+r_k)}{P_d(r)+TP_r(d+r_k)}\frac{\theta_B\theta_U}{4\pi^2}\right)\right]\\ &\overset{(f)}{=}\exp\left(-2\pi\lambda_{BS}\int_0^\infty\right.\\ &\quad\left.\left(1-\exp\left(-\lambda_R\int_{\mathbb{S}^2}\frac{g(r_i,r_k,\psi)TP_r(d+r_k)}{P_d(r)+TP_r(d+r_k)}\frac{\theta_B\theta_U}{4\pi^2}\mathrm{d}r_k\mathrm{d}\psi\right)\right)r_i\mathrm{d}r_i\right),\end{aligned} \tag{20}$$

where r_i is the distance from B_i to the typical user, and r_k is the distance from R_k to the typical user, and ψ is the angle between the B_i to typical user link and the R_k to typical user link. The term $d=\sqrt{r_i^2+r_k^2-2r_ir_k\cos\psi}$ is the distance from B_i to R_k. Equality (c) follows from the i.i.d. distributions of G and h for each link. And in (c), the BSs and RISs in $\tilde{\Phi}_{BS}$ and $\tilde{\Phi}_R$ satisfy $r^{-\alpha}\geq\gamma(d+r_k)^{-\alpha}$, i.e., the path loss of an arbitrary indirect interference link through B_i and R_k is no less than the the path loss of the association direct link with distance r. Equality (d) follows from the distributions of $\mathbb{I}_L(r)$ and $\delta_{B_iR_k}$ and (e) follows from the distribution of G and h. Finally, the equality (f) follows from the probability generating functional (PGFL) of $\tilde{\Phi}_{BS}$ and $\tilde{\Phi}_R$. The distance and angle of the RISs in the region $\mathbb{S}^2$ satisfy $r^{-\alpha}\geq\gamma(d+r_k)^{-\alpha}$ and the R_1 is obtained from this constrain.

References

[1] T. Bai, R. Vaze, and R. W. Heath, "Analysis of blockage effects on urban cellular networks," *IEEE Transactions on Wireless Communications*, vol. 13, no. 9, pp. 5070–5083, 2014.

[2] Huawei Technologies Company, "5G energy white paper," 2019, https://www.huawei.com/minisite/5g-ultra-lean-site-2019/pdf_v1.0/5G-power-cn.pdf.

[3] E. Basar, M. Di Renzo, J. De Rosny, M. Debbah, M.-S. Alouini, and R. Zhang, "Wireless communications through reconfigurable intelligent surfaces," *IEEE Access*, vol. 7, pp. 116 753–116 773, 2019.

[4] M. Di Renzo and J. Song, "Reflection probability in wireless networks with metasurface-coated environmental objects: An approach based on random spatial processes," *EURASIP Journal on Wireless Communications and Networking*, vol. 2019, no. 1, 2019.

[5] C. Zhang, W. Yi, and Y. Liu, "Reconfigurable intelligent surfaces aided multi-cell NOMA networks: A stochastic geometry model," 2020, available online: https://arXiv.org/abs/2008.08457.

[6] T. Hou, Y. Liu, Z. Song, X. Sun, Y. Chen, and L. Hanzo, "MIMO assisted networks relying on intelligent reflective surfaces," 2019, available online: https://arXiv.org/abs/1910.00959.

[7] M. A. Kishk and M.-S. Alouini, "Exploiting randomly-located blockages for large-scale deployment of intelligent surfaces," *IEEE Journal on Selected Areas in Communications*, vol. 39, no. 4, pp. 1043–1056, 2021.

[8] L. Yang, F.-C. Zheng, and S. Jin, "Coverage probability and energy efficiency of reconfigurable intelligent surface-assisted mmwave networks," 2021, available online: https://arXiv.org/abs/2104.07971.

[9] Y. Zhu, G. Zheng, and K.-K. Wong, "Stochastic geometry analysis of large intelligent surface-assisted millimeter wave networks," *IEEE Journal on Selected Areas in Communications*, vol. 38, no. 8, pp. 1749–1762, 2020.

[10] M. Di Renzo, F. H. Danufane, X. Xi, J. De Rosny, and S. Tretyakov, "Analytical modeling of the path-loss for reconfigurable intelligent surfaces–anomalous mirror or scatterer?" in *2020 IEEE 21st International Workshop on Signal Processing Advances in Wireless Communications (SPAWC)*, 2020, pp. 1–5.